

Catalytic Peptide-based Coacervates: Evolutionary Paths for Enhanced Catalytic Function through Structural Organization and Substrate Specificity

Corresponding Author: Dr Ana Pina

This file contains all reviewer reports in order by version, followed by all author rebuttals in order by version.

Version 1:

Reviewer comments:

Reviewer #1

(Remarks to the Author)

This contribution reports an elegant finding, in which a hairpin peptide is found to form coacervates. Of specific interest is that the conformation is stabilized upon coacervation. Furthermore, the peptide has phosphatase activity, which is enhanced in the LLPS phase. This is a novel approach in the area of peptide-based coacervates and is a useful extension of the field of artificial cells, with the possibility to be more generally applicable.

The authors should provide adequate answers to the following comments/questions

Do the coacervates show wetting on the substrate? What is the driving force for division/size decrease?

To understand better the uptake mechanism of the different proteins, the authors should also measure the zeta potential. To determine if charge is the main driving force the authors should study intrinsically negative proteins and analyze their uptake. In this regard, the authors should also provide the isoelectric points of the proteins currently used to study uptake.

Regarding the catalytic activity, is this mainly a local concentration enhancement effect or does the conformational stability of the hairpin also play a role? The authors could study this by synthesizing a locked hairpin.

Furthermore, the authors should determine the local pH in the coacervate phase, which can be assessed with a ratiometric dye.

Do the authors correct for the local substrate concentration? Due to sequestration this could be much higher than in bulk. As such, the K_m value could be overestimated.

There are some other examples of phosphorylation induced uptake in coacervates, see e.g. Veldhuisen et al. Adv Mat 2023. What happens to the phosphorylated proteins? In presence of the catalytic peptide, they could also be dephosphorylated and be released from the coacervate. The authors should investigate if this indeed happens and if not, should provide a rationale for the lack of catalytic activity.

Reviewer #2

(Remarks to the Author)

Reviewer #3

(Remarks to the Author)

The manuscript is a very interesting example of looking at coacervate formation and how the secondary structure of the peptide forming the coacervates can be modified. In this case, this results in an inherent increase in catalytic function. I think there is a lot of very good and interesting high-impact work presented in the manuscript, for example the substrate sequestration of the different enzymes and the use of a catalytic peptide to add function to the coacervate, unfortunately the conclusions are not fully supported by the experiments. I believe if the authors can realize a few control experiments the manuscript would be ready to be published in Nature communications.

Major issue:

1) The authors claim that the secondary structure change of the peptide towards more hairpin, as followed through the CD

spectroscopy, is in large part the mechanistic improvement pathway. I would first have the authors explain how the results were normalized to the varying peptide concentrations (this goes for the CD, kinetics, etc). Secondly, there are many other variables that might be changing the catalytic properties of the peptide, yet no adequate control have been realized or proposed by the authors.

- a. A coacervate be formed with a secondary non-catalytic peptide that is then spiked with the P7 peptide. The P7 could therefore be at the same concentration as the bulky solution but the confirmation would be different.
 - b. Could buffer conditions (viscosity, etc) be optimized to show the conformational change of the P7 and improvement in kinetics.
 - c. In general the autocatalysis of the substrate in the coacervate needs to be demonstrated. Again a non-catalytic coacervate peptide should be chosen for this control.
- 2) I would like to see a bit more temperature data the 23 and 27 C seems like two arbitrary data points for the coacervation studies. Similarly, the kinetics at different temperatures would be beneficial.
 - 3) For the supplementary info in part 3 where you are looking at the partitioning. I think the result is really interesting, but it does seem like different enzyme/dye to peptide ratios need to be studied for a proper analysis.

Minor issues:

- 1) Can the aggregates be tested for catalytic activity?
- 2) There are some formatting issues, particularly when equations are involved with subscript, etc.
- 3) I think the authors overplay some phrases in the introduction. For example: "In any event, the potential use of peptides to induce coacervate formation is yet to be fully recognized." is pretty silly when there are special issues dedicated to the topic and all sorts of publications coming out all the time. I would ask that the authors reconsider some of the hyperbole.
- 4) In a similar vein, I feel the work of the Elbaum-Garfinkle and Ulijn groups in peptide coacervates has been overlooked. I recommend the authors look at:
 - a. <https://onlinelibrary.wiley.com/doi/full/10.1002/anie.202218067>
 - b. <https://www.sciencedirect.com/science/article/pii/S245192942200153X>
 - c. <https://onlinelibrary.wiley.com/doi/abs/10.1002/ange.202311479>
 - d. <https://www.nature.com/articles/s41467-020-18224-y>

Reviewer #4

(Remarks to the Author)

This is an interesting study with great potential. However, there are several concerns that need to be addressed.

- 1) Applicability of CD for structural analysis of aggregated protein samples and samples that underwent LLPS is questionable. Results are undoubtedly affected by light scattering. Therefore, reported spectral shapes (and the complete lack of signal for aggregated protein) should not be used for any structural interpretations.
- 2) Instead, alternative approaches (e.g. FTIR), which are not sensitive to the artifacts generated by aggregation, should be used for structural characterization of E7 peptide under the variety of conditions.
- 3) More focus should be given to NMR-based analyses.
- 4) Sequence of the analyzed peptide is rather hydrophobic. Potentially, it never exists as a monomer. Some analysis of the association state of the "soluble" sample should be conducted.
- 5) There is no any evidence showing that P7 has a flexible hairpin-like structure in soluble form. Formation of a fully folded β -hairpin structure is not supported by data provided.
- 6) What was phosphorylation degree of proteins used in this study?
- 7) The authors mentioned that in their experiments on the catalytic efficiency, no observable hydrolysis of pNPP occurred even after 90 hours was found without coacervation. However, previous study showed that this peptide is catalytically active "in a bulk solution under catalytic optimal conditions". The authors should indicate what is the difference between the conditions used in their study and previously reported "catalytic optimal conditions". Can coacervates be formed at these "catalytic optimal conditions"?

Version 2:

Reviewer comments:

Reviewer #1

(Remarks to the Author)

The authors have extensively and adequately answered all the reviewers' comments. The paper is now suited for publication

Reviewer #2

(Remarks to the Author)

The authors have addressed all my comments and concerns in their revision. I would now recommend publication.

Reviewer #3

(Remarks to the Author)

I commend the authors for undertaking considerable work to improve the manuscript and to make things clearer to a reader, where pertinent they have realized the suggested experiments and where not feasible they have provided an adequate explanation. I believe the manuscript is ready to be accepted for publication.

Reviewer #4

(Remarks to the Author)

All my concerns were adequately addressed, and the manuscript was revised accordingly. I do not have new queries.

Open Access This Peer Review File is licensed under a Creative Commons Attribution 4.0 International License, which permits use, sharing, adaptation, distribution and reproduction in any medium or format, as long as you give appropriate credit to the original author(s) and the source, provide a link to the Creative Commons license, and indicate if changes were made.

In cases where reviewers are anonymous, credit should be given to 'Anonymous Referee' and the source.

The images or other third party material in this Peer Review File are included in the article's Creative Commons license, unless indicated otherwise in a credit line to the material. If material is not included in the article's Creative Commons license and your intended use is not permitted by statutory regulation or exceeds the permitted use, you will need to obtain permission directly from the copyright holder.

To view a copy of this license, visit <https://creativecommons.org/licenses/by/4.0/>

Point by point responses to the reviewers' comments:

Reviewer #1

This contribution reports an elegant finding, in which a hairpin peptide is found to form coacervates. Of specific interest is that the conformation is stabilized upon coacervation. Furthermore, the peptide has phosphatase activity, which is enhanced in the LLPS phase. This is a novel approach in the area of peptide-based coacervates and is a useful extension of the field of artificial cells, with the possibility to be more generally applicable. The authors should provide adequate answers to the following comments/questions.

Response: We thank the reviewer for the positive feedback. Please see our responses for each of the comments below.

1. Do the coacervates show wetting on the substrate? What is the driving force for division/size decrease?

Response: Thank you for this insightful question. We have indeed observed that the P7 peptide coacervates can show some wetting on glass substrates. To mitigate this effect and ensure consistent coacervate formation, we functionalize the glass substrate with a 1% Pluronic solution, as described in the Methods section under 'Coacervation'. This functionalization helps maintain the spherical shape of the coacervates and reduces substrate interactions.

Regarding the driving force for division and size decrease, our studies have revealed that temperature plays a crucial role in the coacervation process of the P7 peptide. We investigated temperatures ranging from 23°C to 37°C and found that temperatures above 27°C led to higher turbidity values (Figure S3), favoring coacervate formation compared to temperatures below 25°C (Figure S4). In our study, the samples were initially incubated at 27°C to induce coacervation and then maintained at room temperature (23°C ± 2°C) for 6 hours. This cooling process likely impacts the coacervate stability and dynamics, contributing to the observed changes in size and number. The interplay between temperature-dependent hydrophobic interactions and the liquid-like nature of the coacervates likely drives the observed division and size decrease phenomena.

To clarify this point, we added the following text to the revised manuscript (page 9, lines 174-185): Furthermore, we also characterized the temporal dynamics of the coacervation process through time-course analysis. The samples were initially incubated at 27°C to induce coacervation and subsequently maintained at room temperature (23°C ± 2°C) for a total duration of 6 hours. This analysis revealed that while the coacervates had a larger size at one-hour coacervation, their size gradually decreased over time due to the formation of liquid bridges, leading to an increased number of coacervates (Figure S5). This phenomenon is characteristic of liquid-like condensates, which can fuse, deform or, as in this case, split into two coacervates. This cooling process from 27°C to room temperature seems to impact coacervate dynamics. These temperature-dependent changes appear to contribute significantly to the observed division and size decrease of the coacervates. The observed coacervate size range was consistent with values reported in the literature, typically 1-10 μm¹⁸. This size range of the coacervates also corroborated by dynamic light scattering (DLS) (Figure S6).

2. To understand better the uptake mechanism of the different proteins, the authors should also measure the zeta potential. To determine if charge is the main driving force the authors should study intrinsically negative proteins and analyze their uptake. In this regard, the authors should also provide the isoelectric points of the proteins currently used to study uptake.

Response: We appreciate the reviewer's suggestion and we have conducted dynamic light scattering measurements to address this point. The zeta potential of P7 undergoing LLPS (stock concentration 5 mg/mL in 100 mM sodium phosphate buffer, pH 8.0, 1M NaCl) was determined to be $+9.4 \pm 3.2$ mV. This positive value aligns with expectations based on the peptide's isoelectric point (pI 11.46), confirming that the P7 coacervates indeed have a net positive surface charge.

To investigate whether charge is the primary driving force for protein uptake, we investigated the isoelectric point of the proteins used in this study:

CotB: Intrinsically positive (pI 9.83)

BSA: Intrinsically negative (pI 5.6-6.0)

Tau: Intrinsically negative (pI 6.2-6.25)

Our results show that the non-phosphorylated forms of these proteins (Figure 4), regardless of their intrinsic charge, are excluded from the coacervates and remain confined to the boundaries even after a 3-hour incubation period. This observation is particularly noteworthy for the negatively charged BSA and Tau, which might be expected to interact electrostatically with the positively charged coacervates.

In contrast, the phosphorylated forms of these proteins are effectively sequestered within the coacervates. This selective uptake occurs despite the additional negative charges introduced by phosphorylation, which would theoretically increase electrostatic repulsion with the positively charged coacervate surface.

These findings strongly suggest that charge is not the primary driving force for protein sequestration within the coacervates. Instead, our results indicate that the molecular recognition capabilities of the peptide sequence towards phosphorylated assemblies play a crucial role in the uptake mechanism.

To clarify this point, we added the following text to the revised manuscript:

(Page 10, lines 250-251): At pH 8.0, the P7 coacervates present a net positive surface charge of $+9.4 \pm 3.2$ mV as determined by dynamic light scattering (DLS) measurements.

(Page 12, lines 296-298): BSA, Tau, and all their phosphorylated versions are intrinsically negative due to their isoelectric points and degrees of phosphorylation. In contrast, CotB is intrinsically positive (Table S3).

Supplementary Table 3- Isoelectric points of the P7 and the proteins used in the affinity-mediated molecular uptake study

Proteins	Isoelectric Point
P7 peptide	11.46 (estimated by using Pepcalc tool)
BSA	5.6-6 (at pH 8 is intrinsically negative)
Tau	6.25 (at pH 8 is intrinsically negative)
CotB	9.83 (at pH 8 is intrinsically positive)
CotBp	4.51

(Page 12, lines 305-316): This selective uptake is particularly noteworthy given that BSA and Tau are intrinsically negatively charged proteins, which might be expected to interact electrostatically with the positively charged coacervate surface. These findings strongly suggest that electrostatic interactions are not the primary driving force for protein sequestration within the coacervates. Instead, our results indicate that the selective binding properties of the P7 peptide sequence towards phosphorylated assemblies¹ play a crucial role in the uptake mechanism, as demonstrated by the preferential uptake of phosphorylated proteins over their non-phosphorylated counterpart¹. This phosphate-specific recognition suggests that it may be possible to incorporate other molecular recognition capabilities towards specific targets within the sequences of phase-separating peptides, paving the way for the creation of a novel class of functional biomolecular coacervates capable of mediating selective molecular uptake, resembling the processes observed in cellular functions.

The materials and methods section were also updated accordingly with this new data, and we added the following text:

Dynamic Light scattering: The size of coacervates and their zeta potential was measured by dynamic laser scattering (DLS) (Malvern Zeta-sizer Nano ZS). For size measurements, P7 samples with the different assembly states (soluble with low turbidity, undergoing LLPS and aggregated state) were induced for a final volume of 2mL. Furthermore, 500uL of each sample was transferred to 1.5mL SARSTEDT disposable cuvettes and proceeded to size measurements. Lastly, for the measurement of the zeta potential, we transferred 700uL from the stock solutions to ZETASIZER NANO SERIES disposable folded capillary cells. The experiments were performed in triplicates.

3. Regarding the catalytic activity, is this mainly a local concentration enhancement effect or does the conformational stability of the hairpin also play a role? The authors could study this by synthesizing a locked hairpin.

Response: We are grateful for the reviewer's valuable suggestion. We believe that the primary factor influencing the catalytic activity is the structural plasticity of the peptide P7, which leads to the formation of dynamic coacervates through liquid-liquid phase separation (LLPS). This process provides a unique conformational stabilization that is crucial for the enhanced catalytic efficiency observed. Regarding the suggestion to synthesize a locked hairpin, we acknowledge its potential as a strategy to stabilize P7 conformation. However, we believe that such an approach would introduce rigidity into the system, potentially compromising the structural plasticity and dynamics of P7. This flexibility is essential for the peptide's ability to undergo LLPS and form functional coacervates.

A synthetic locked hairpin, while potentially offering increased stability, might inhibit these beneficial dynamic properties. The rigidity could impair the peptide's ability to form functional coacervates and adapt to the LLPS environment, potentially reducing overall catalytic efficiency.

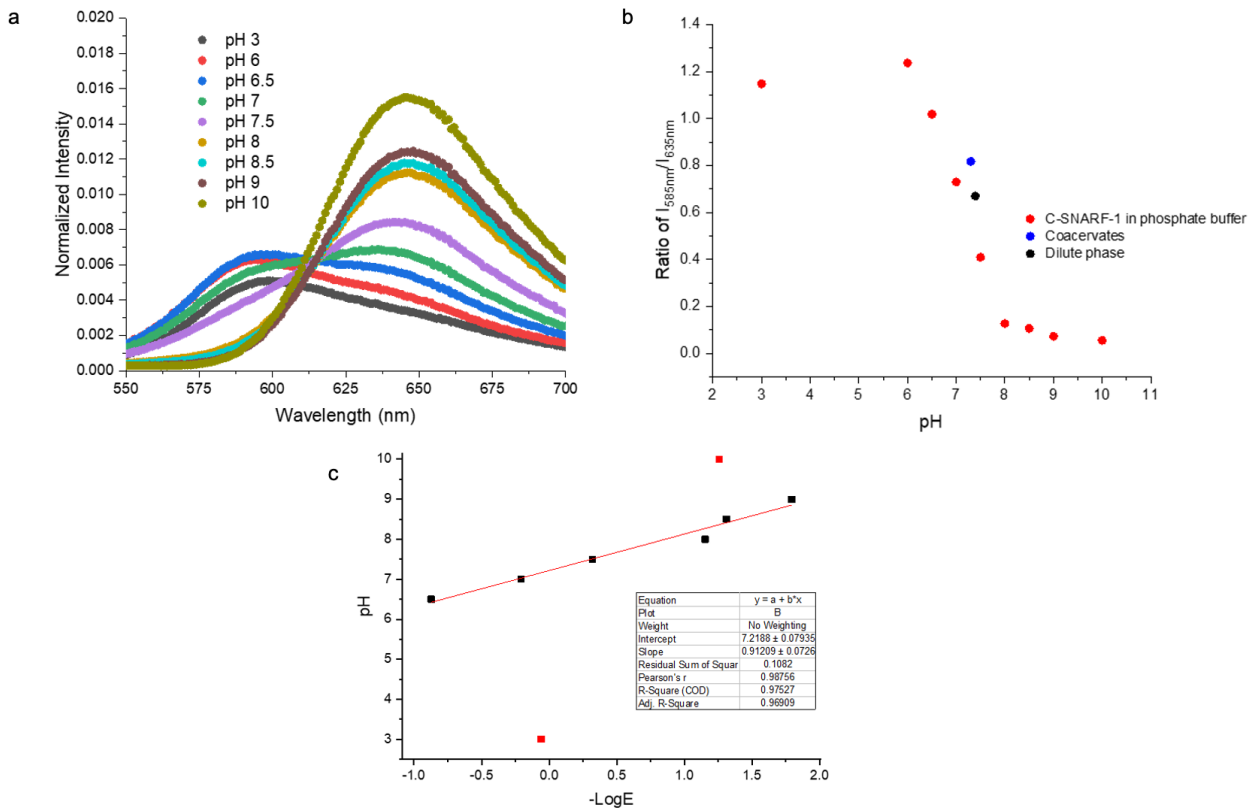
We greatly appreciate this suggestion and consider it valuable for future investigations. In subsequent studies, we plan to explore the impact of varying degrees of conformational constraint on catalytic activity. This approach will allow us to further elucidate the relationship between structural flexibility and catalytic efficiency in our system.

4. Furthermore, the authors should determine the local pH in the coacervate phase, which can be assessed with a ratiometric dye.

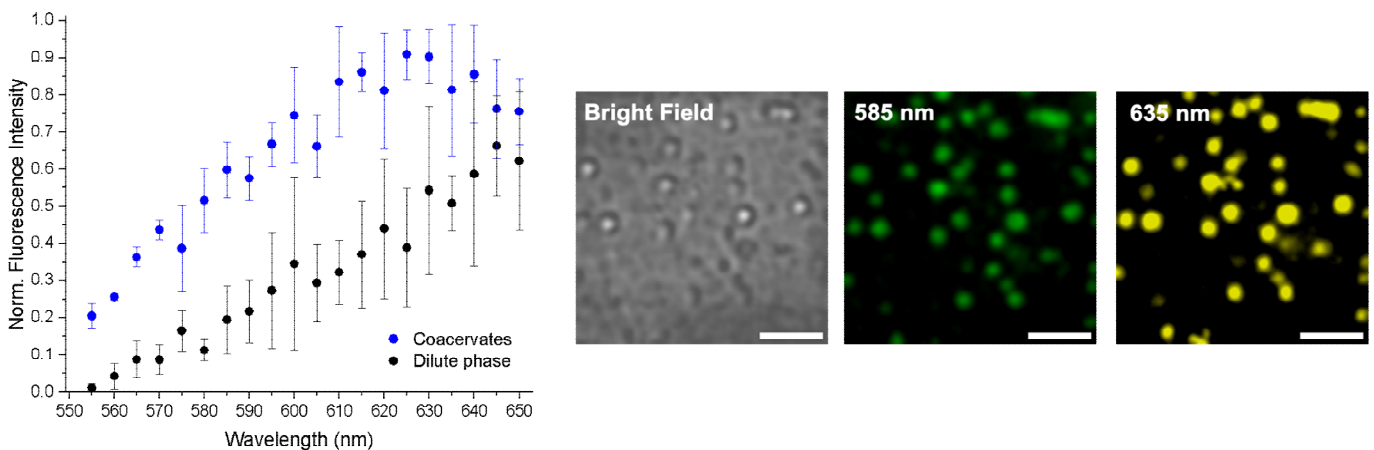
Response: We thank the reviewer for the suggestion. We have determined the local pH in the coacervate phase by following the methodology described by the Christine Keating group^{2,3} to assess the apparent pH inside the coacervate droplets. For this, we used the ratiometric pH indicator dye 5-(and 6)-carboxy SNARF-1 (SNARF), which has dual fluorescence emission peaks that change depending on the dye's protonation state and is commonly used to determine local pH in microenvironments such as condensate phases. First, we performed a calibration curve of the emission spectra of SNARF from 560 to 700 nm in various pH solutions according to the supplier's (Thermo) instructions and the protocols described by the Keating group. The local apparent pH of both the coacervate phase and dilute phases was estimated using a lambda scan with confocal microscopy. The apparent pH in the coacervate phase was approximately 7.3, while in the dilute phase it was around 7.4. This indicates that there were no significant changes in pH between the dilute and condensed phases, and the coacervates remained positively charged.

To clarify this point, we added the following text to the revised manuscript (page 10, lines 250-256) and the new figures in supplementary section:

Local apparent pH inside coacervate droplets and the dilute phase was measured using 5-(and 6)-carboxy SNARF-1 (SNARF), a pH-sensitive indicator dye, as described by the Keating group^{2,3}. By partitioning SNARF-1, we were able to measure the local apparent pH of both the coacervate phase and the dilute phase, which were estimated to be approximately 7.3 and 7.4, respectively. (Supplementary section 3 – Figures S10 and S11).



Supplementary Figure 10: Calibration methods of SNARF to estimate local apparent pH. (a) The fluorescence spectra of SNARF collected across a range of pH values. (b) Ratio of SNARF intensity at 585 nm and 635 nm as a function of pH changes. (c) pH calibration curve for SNARF-1 fluorescence. The pH is plotted against $-\log E$, where $E = (R-RB) / (RA-R)$. R represents the ratio of SNARF-1 fluorescence intensities at 585 nm and 635 nm. RA and RB are the ratio of SNARF fluorescence intensity at 585 nm and 635 nm at acidic and basic pH extremes, respectively. pH estimation was performed following established protocols



Supplementary Figure 11: Confocal images and lambda scan of SNARF in coacervate droplets. SNARF emission spectrum in coacervate droplets and dilute phase are measured by confocal microscope simultaneously and used to estimate the local apparent pH of SNARF

The materials and methods section were also updated accordingly with this new data, and we added the following text:

Local Apparent pH Measurement: Local apparent pH measurements were performed following the method described by Keating *et al*^{2, 3}. SNARF-1 was prepared at a stock concentration of 300uM in ultrapure water. For the calibration curves, SNARF-1 emission spectra were collected across the range of 500 to 700 nm in various pH solutions, using an excitation wavelength of 514 nm. The pH of the calibration solution was adjusted by addition of NaOH or HCl solutions and measured by using the pHenomenal pHmeter (VWR). For coacervate samples, SNARF-1 emission spectra were measured within and outside coacervate droplets using a lambda scan on a Zeiss LSM 880 laser scanning confocal microscope, covering the range of 555-700 nm. Excitation was provided by a 514 nm laser, with a 20% laser intensity and 500–800 V gain. Imaging of the coacervates was performed using a 63x Plan-Apochromat 1.4 NA DIC oil immersion objective (Zeiss). The microscope was controlled using Zeiss Zen 2.3 (black edition) software. The lambda scan was collected with a 5 nm step size and 10 nm bandwidth. Five ROIs per image were collected to estimate the local apparent pH of coacervate droplets. Image analysis was conducted using Zeiss Zen 2.3 (black edition) software and ImageJ/FIJI⁴.

5. Do the authors correct for the local substrate concentration? Due to sequestration this could be much higher than in bulk. As such, the Km value could be overestimated.

Response: The authors acknowledge the important comment and have clarified the analysis of the kinetic data and performed partitioning experiments with the substrate pNPP. To address the reviewer's concern about local substrate concentration, we provide the following clarifications:

- Kinetic data analysis: The analysis of kinetic experiment data conducted with P7 coacervates was done by subtracting the absorbances of P7 coacervates without pNPP and the absorbances over time of pNPP autohydrolysis in bulk. This approach helps account for background effects and isolates the catalytic activity of the coacervates.
- pNPP sequestration estimation: To better estimate pNPP sequestration within the coacervates, we carried out partitioning assays. The partition efficiency was calculated by measuring the absorbance of pNPP at 312 nm. Results showed that the partitioning efficiency ranged from 8-18%, depending on the pNPP concentration.
- Local substrate concentration: The partitioning efficiency results indicate that pNPP sequestration inside the coacervates is not significantly higher than in bulk solution. Given the relatively partitioning efficiency of 8-18%, it is unlikely that the Km value is significantly overestimated due to substrate sequestration.

To clarify this point, we added the following text to the revised manuscript in the section of the materials and methods under the section **Kinetic experiments of P7 the materials and methods** (Page 21, lines 610-634): The analysis of kinetic experiment data conducted with P7 coacervates involved two key corrections: (1) to account for the turbidity interference caused by coacervates, the absorbances of P7 coacervates without pNPP were subtracted from the experimental readings, and (2) to account for the autohydrolysis of the substrate in bulk solution, the absorbances of pNPP over time (without coacervates) were also subtracted from the experimental readings. These corrections allowed for a more accurate assessment of the catalytic activity of P7 coacervates by isolating the pNPP hydrolysis specifically caused by the peptide-based coacervates.

The new data to support Local substrate concentration analysis the was also added in:

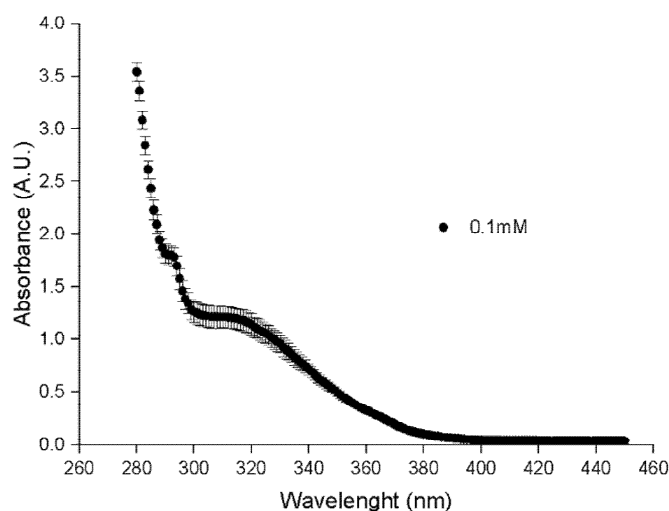
Page 14, lines 347-351: To better estimate pNPP sequestration within the coacervates, the encapsulation efficiency of pNPP was determined, showing an efficiency ranging from 8-18%, depending on the pNPP concentration (Figs. S21 and S22). These results indicate that pNPP sequestration inside the coacervates is not significantly higher than in the bulk solution.

Page 15 in the supporting information in the “catalytic efficiency of the P7 based coacervates” section:

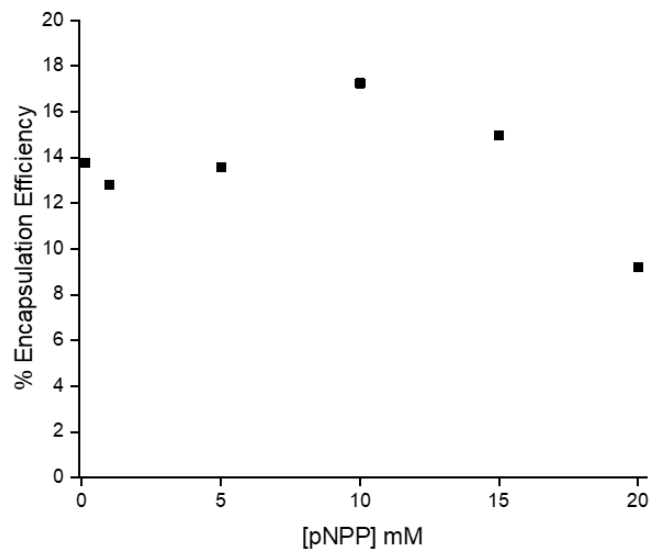
The partitioning efficiency of the substrate pNPP inside the coacervates was investigated and for this the absorbance spectra of pNPP were analyzed, revealing a peak at 312 nm (Fig. S21).

pNPP Absorbance Spectra: A solution of 275 μ L of 100 mM sodium phosphate with 1 M NaCl at pH 8.0 was prepared. To this, 25 μ L of pNPP was added to achieve a final concentration of 0.1 mM, with a pNPP to solution ratio of 1:12. The sample's absorbance was then measured using the INFINITE M NANO+ TECAN microplate reader, scanning from 250 to 450 nm. A distinct absorbance peak was observed at 312 nm, corresponding to the pNPP absorbance.

The partitioning protocol was then performed as described in the "Partitioning Experiments" section for the different final concentrations of pNPP (1-20 mM) used in the kinetic experiments.



Supplementary Figure 17 Absorbance spectra of the pNPP



Supplementary Figure 18 Encapsulation efficiency (%) as a function of the pNPP concentration inside P7 coacervates. The encapsulation efficiency was determined by measuring the partitioning of the pNPP within the coacervates. Data are presented as mean values \pm SD (n=3).

6. There are some other examples of phosphorylation induced uptake in coacervates, see e.g., Veldhuisen et al. Adv Mat 2023. What happens to the phosphorylated proteins? In presence of the catalytically peptide, they could also be dephosphorylated and be released from the coacervate. The authors should investigate if this indeed happens and if not, should provide a rationale for the lack of catalytic activity.

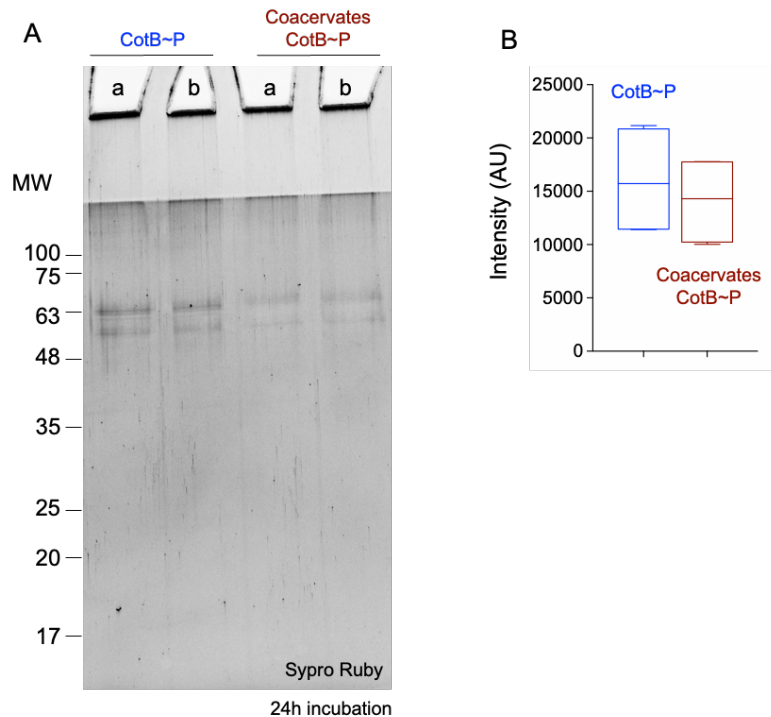
Response: The authors acknowledge the insightful comment. We thank the reviewer for bringing this relevant work to our attention. Indeed, van Veldhuisen et al. (Adv. Mat. 2023) have demonstrated phosphorylation-induced uptake in coacervates, which can complement our findings. In this way, we have included this work in the manuscript for reference. We have added the following text to the revised manuscript (page 13, lines 318-320)

Similarly, van Veldhuisen *et al.* have shown the selective recruitment of phosphorylated binding partners into coacervates, highlighting the role of phosphorylation in mediating specific protein-protein interactions within coacervates⁵.

Regarding the second part of the comment, while coacervates have been shown to selectively bind phosphorylated proteins, their ability to promote their dephosphorylation appears limited, with the primary focus being on small, phosphorylated molecules. Nevertheless, we have investigated the capability of the P7 coacervates to dephosphorylate proteins. Among the three proteins studied in this manuscript—BSA_p, Tau_p, and CotB_p—we selected CotB_p for further studies. The rationale is that BSA_p is a very stable globular protein, even resistant to trypsin, and the potential phosphoryl-acceptor sites may not be exposed. Tau_p is an intrinsically disordered protein that tends to aggregate upon phosphorylation, forming plaques that can hinder enzymatic action. In contrast, CotB_p is poly-phosphorylated at serine residues located in a long C-terminal tail, predicted to be intrinsically disordered. Moreover, this region of the protein is rapidly dephosphorylated by alkaline phosphatase⁶. We incubated the P7 coacervates with CotB_p for 24 hours and assessed the dephosphorylation pattern using densitometric

analysis of electrophoretically resolved proteins after staining the gels with Pro-Diamond Q (Q), which stains inorganic phosphate, and with Sypro Ruby (S) to stain the total protein in the gel. We analyzed the samples at 24 hours for both the P7 coacervates with CotBp and the respective controls, which included a parallel incubation of CotBp in the absence of coacervates. We expected the Q/S ratio to decrease. As evidenced by the Sypro Ruby stain (Fig. RRL1), incubation of CotBp with coacervates results in a notable decrease in the total protein signal (S). This reduction leads to a partial disappearance of the CotBp band. The same profile was also observed for the inorganic phosphate stained with Pro-Diamond Q. Consequently, the quantification of the Q/S signal becomes potentially misleading, making it challenging to accurately infer the phosphorylation state of CotB under these conditions. This observation suggests that the interaction between CotBp and the coacervates may be altering the protein's behavior or detectability in the gel, complicating the interpretation of its phosphorylation status.

One possibility is that the unphosphorylated protein (CotB), after incubation with P7 coacervates and subsequent dephosphorylation, may form aggregates that are not resolved by SDS-PAGE. When expressed in *E. coli*, CotB, but not CotBp, accumulates in inclusion bodies⁶. We are loading a total (unfractionated) sample, and we do see material at the well and at the stacking/resolving gel interface (figure below). However, we do not see differences between the protein alone or in the presence of coacervates. Another possibility, which seems closer to the results, is that CotBp is unstable in the presence of the coacervates. In any event, we were unable to quantify the total amount of unphosphorylated protein in this assay.



Reviewer Response Letter Figure 1: Sypro Ruby staining of CotBp and P7 coacervates with CotBp after 24 hours incubation. **A.** The gel shown is representative of the Sypro Ruby staining obtained for the indicated samples (two replicates, *a* and *b*, are shown). molecular weight markers, in kDa, on the left side of the panel. **B.** Quantification of the signal in each lane of the indicated samples. Four different lanes for each sample

were quantified using ImageJ, after imaging the gel with a laser scanning instrument (Fuji TLA-5100) using an excitation at 488 nm and a long-pass emission filter.

We also attempted NMR and MS analyses, but these were inconclusive due to the high salt content in the samples, which interfered with NMR analysis, and the heterogeneity of the samples, which precluded the MS analysis. Given that these results require an extensive analysis of the dephosphorylation profile of CotBp in the presence of coacervates, we have opted to exclude these findings from the main manuscript. This decision was made to maintain focus on the core findings and to avoid presenting potentially inconclusive data without a comprehensive investigation. Further studies are planned to elucidate the complex interactions between CotBp, its dephosphorylation, and coacervate formation.

Reviewer #2

In this manuscript, the authors investigate the role of LLPS in enhancing the catalytic efficiency and substrate specificity of peptide P7. They showed that LLPS mediated droplets not only exhibit a 15000-fold in enzymatic activity compared to non-phase separated soluble peptides but can also selectively sequester phosphorylated substrates compared to non-phosphorylated substrates. In the course their research, they used a combination of enzyme catalysis studies and biophysical techniques including light scattering, microscopy, CD and NMR spectroscopy. They show that the self-coacervation of peptide P7 is reversible and is dependent on solution conditions such as salt concentration and P7 concentration. However, under certain conditions, aggregates form. Their CD spectroscopy experiments demonstrate some conformational transition changes from a flexible disordered structure to beta-hairpin conformation. The changes in NMR spectroscopy chemical shift changes also reflect some conformational changes accompanying phase separation. To investigate the milieu formed within these P7 droplets, the authors investigated the sequestration and dynamics of aromatic dyes rhodamine, FITC and DAPI as well as GFP. They showed that less hydrophobic and negatively charged dyes as well as phosphorylated substrates are more encapsulated within the P7 coacervates. Taken together, the authors demonstrate the ability of peptides to form both membrane-less droplets and to catalyze reactions with enhanced activity and selectivity. This paper will be of interest to the general readers of Nature Communication.

General Comments: The manuscript was well-written and organized, and straight forward to read and follow. In the attached documents, I have included specific comments to help improve the documents.

Response: We sincerely appreciate the reviewer's thoughtful feedback and constructive comments. We have carefully addressed each point raised, and our detailed responses to the specific comments are provided below.

1. I have only one major issue concerning the interpretation of the CD and NMR spectroscopy results. On line 97-99 of the manuscript, the authors wrote "Then, we demonstrate that coacervation reduces the conformational flexibility of the peptide, stabilizing a fully folded β -hairpin structure". However, if there was there such significant structural change upon phase separation, the NMR chemical shift changes would have been more dramatic. I think without performing assignment experiments of the two states, it will be very difficult to just that statement. It's feasible that the CD is detecting only partial folded Beta-hairpin structures.

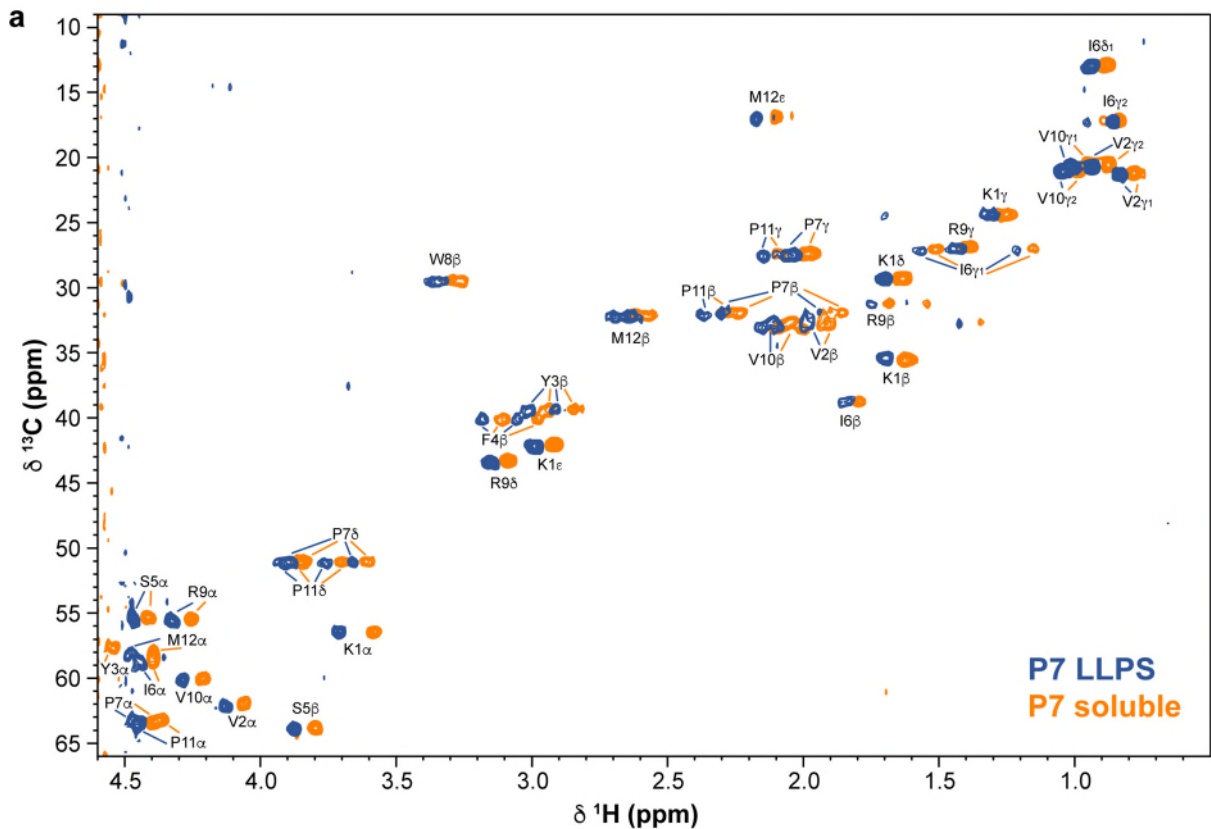
Response: As suggested by the reviewer, the NMR data was analyzed in more detail. For a more distinctive comparison with the undergoing LLPS state, spectra were acquired at 5 mg ml⁻¹ and no salt as a representative condition for the soluble low turbidity and small amount of coacervates state. Assignments were performed for both conditions

(soluble state - 5 mg ml⁻¹ in 100mM sodium phosphate buffer pH 8.0 with no NaCl (in orange); LLPS state - 5mg mL⁻¹ in 100mM sodium phosphate buffer pH 8.0 and 1 M of NaCl), and the secondary structure propensity was calculated with the CSI 3.0 web server. For the soluble state, a turn and a random coil stretch was determined, and for the LLPS state a turn within a beta-strand and a random coil region that corroborates the formation of a beta-hairpin structure. The data does not allow solving the structure of the peptide in these states, since the pH of the experiments (pH 8), almost no NH connectivities are observed. These new results were included and discussed in Section *LLPS can induce reversible self-coacervation of peptides with conformational flexibility* and Supplementary Figure 7 was updated and a table with backbone assignments was added (Supplementary Table 1).

To clarify this point, we added the following text to the revised manuscript (page 8, lines 192-202) and a new table (Supplementary Table 1) and figure (Supplementary Figure 7) in the supplementary information: **Our results suggest that LLPS induces the stabilization of the secondary structure of P7, transforming a flexible hairpin-like peptide in solution into a fully folded β -hairpin structure in the LLPS state. In fact, NMR analysis for the soluble and undergoing LLPS assembly states corroborate these findings. The secondary structures propensities calculated from the assigned chemical shifts (Table S1) revealed a beta-hairpin in LLPS state compared with a flexible hairpin-like peptide structure in the soluble state as showed by the presence of a turn within two random coil stretches (Figure S7).**

Supplementary Table 1 – P7 assigned backbone chemical shifts in the soluble and undergoing LLPS states. The chemical shifts were used for determination of the secondary structure elements represented in Supplementary Figure 7. Soluble state - 5 mg ml⁻¹ in 100mM sodium phosphate buffer pH 8.0 with no NaCl; LLPS state - 5mg mL⁻¹ in 100mM sodium phosphate buffer pH 8.0 and 1 M of NaCl

Residue	P7 soluble				P7 LLPS			
	HA	CA	CB	HN	HA	CA	CB	HN
K1	3,710	56,59	35,44	-	3,554	56,51	35,58	-
V2	4,129	62,23	32,70	-	4,060	62,08	32,87	-
Y3	4,610	-	39,44	-	4,542	57,72	39,33	-
F4	4,700	-	40,14	-	4,638	-	40,14	-
S5	4,469	55,36	63,99	-	4,403	55,39	63,90	-
I6	4,437	58,89	38,84	8,147	4,393	58,85	38,81	-
P7	4,455	63,36	32,01	-	4,390	63,41	31,98	-
W8	4,723	-	29,56	7,950	4,651	57,27	29,42	7,997
R9	4,324	55,64	31,33	-	4,255	55,54	31,24	-
V10	4,284	60,18	32,96	8,042	4,212	60,09	32,85	8,001
P11	4,449	63,57	32,21	-	4,367	63,25	31,95	-
M12	4,474	58,30	32,25	-	4,401	58,02	32,07	-



Supplementary Figure 7 – NMR studies on P7 coacervation. (a) 2D ^1H , ^{13}C HSQC spectra and assignments for the two conditions analyzed: P7 peptide in a stock concentration of 5mg mL^{-1} in 100mM sodium phosphate buffer with no salt (soluble, in orange) and 1 M of NaCl at $\text{pH } 8.0$ (undergoing LLPS, in blue); (b) secondary structure graph as determined by CSI 3.0 web server with the backbone chemical shifts shown in Table S1.

The materials and methods section were also updated accordingly with this new data, and we added the following text:

NMR Samples preparation and experiments: For NMR studies the P7 peptide samples were prepared according to the coacervation protocol described as in supplementary note 2 in soluble with low turbidity and undergoing LLPS states. The conditions prepared were P7 peptide in a stock concentration of 5mg mL^{-1} in 100mM sodium phosphate buffer with no salt (soluble) and 1 M of NaCl at $\text{pH } 8.0$ (undergoing LLPS) in $92\% \text{H}_2\text{O}/8\% \text{D}_2\text{O}$.

NMR experiments were acquired either at FCT-NOVA or ITQB in Bruker Avance Neo 500 MHz spectrometers equipped with a 5 mM triple resonance Prodigy cryoprobe (TCI). 2D ^1H TOCSY (40 ms), 2D ^1H ROESY (250 ms) and 2D ^1H , ^{13}C HSQC spectra were acquired at $23\text{ }^\circ\text{C}$ and processed using TopSpin (Bruker Biospin) and analyzed with POKY⁷ for assignment. Secondary structure elements were determined with the CSI 3.0 web server⁸.

2. Maybe if the authors can speculate about the origin of the substrate specificity for phosphorylated vs non-phosphorylation substrates, that would be great. I think this manuscript should be considered for publication after addressing these.

Response: We appreciate the reviewer's insightful suggestion and have revised the text to address the origin of substrate specificity for phosphorylated versus non-phosphorylated substrates.

The P7 peptide was discovered through the selection of a peptide-based phage display library targeting phosphorylated assemblies described by Pina et al¹. This selection utilized supramolecular tyrosine-phosphate ligands represented by 9-fluorenylmethoxycarbonyl-phenylalanine-tyrosinephosphate (Fmoc-FpY) micellar aggregates as targets. Since the peptide was specifically selected for its binding affinity towards phosphorylated assemblies, its interaction is highly dependent on the presence of phosphorylation. When binding experiments were conducted with the non-phosphorylated target (Fmoc-FY), no binding was observed. This lack of interaction underscores the substrate specificity of the P7 peptide, which originates from its selection process geared towards phosphorylated assemblies. The peptide's ability to recognize and bind phosphorylated targets is a direct result of this selection, highlighting the critical role of phosphorylation in dictating the peptide's binding specificity.

To clarify this point, we have revised the text (page 12, lines 306-317):

This selective uptake is particularly noteworthy given that BSA and Tau are intrinsically negatively charged proteins, which might be expected to interact electrostatically with the positively charged coacervate surface. These findings strongly suggest that electrostatic interactions are not the primary driving force for protein sequestration within the coacervates. Instead, our results indicate that the selective binding properties of the P7 peptide sequence towards phosphorylated assemblies¹ play a crucial role in the uptake mechanism, as demonstrated by the preferential uptake of phosphorylated proteins over their non-phosphorylated counterpart¹. This phosphate-specific recognition suggests that it may be possible to incorporate other molecular recognition capabilities towards specific targets within the sequences of phase-separating peptides, paving the way for the creation of a novel class of functional biomolecular coacervates capable of mediating selective molecular uptake, resembling the processes observed in cellular functions.

Reviewer #3 (Remarks to the Author):

The manuscript is a very interesting example of looking at coacervate formation and how the secondary structure of the peptide forming the coacervates can be modified. In this case, this results in an inherent increase in catalytic function. I think there is a lot of very good and

interesting high-impact work presented in the manuscript, for example the substrate sequestration of the different enzymes and the use of a catalytic peptide to add function to the coacervate, unfortunately the conclusions are not fully supported by the experiments. I believe if the authors can realize a few control experiments the manuscript would be ready to be published in Nature communications.

Response: We thank the reviewer for the positive feedback. Please see our responses for each of the comments below.

1) The authors claim that the secondary structure change of the peptide towards more hairpin, as followed through the CD spectroscopy, is in large part the mechanistic improvement pathway. I would first have the authors explain how the results were normalized to the varying peptide concentrations (this goes for the CD, kinetics, etc). Secondly, there are many other variables that might be changing the catalytic properties of the peptide, yet no adequate control have been realized or proposed by the authors.

Response: We thank the reviewer for this important comment. We acknowledge that the experimental protocol of CD and kinetics data in its original version might not be clear enough and would like to clarify this. Regarding **the CD analysis**, after obtain the CD spectra in millidegrees, we have subtracted the buffer baseline, and the ellipticity was calculated by using the following formula $[\theta] = \text{millidegrees} / (\text{pathlength of the cell} \times \text{the molar concentration of protein} \times \text{the number of residues})$, according to the literature⁹. To clarify our experimental protocols for the CD data, the materials and methods section were also updated and we added the following text:

For the CD measurements, quartz cuvettes with a path length of 0.1 cm were used for the P7 peptide stock solution at 1 mg mL⁻¹, while cuvettes with a path length of 0.01 cm were used for the 5 mg mL⁻¹ and 10 mg mL⁻¹ P7 peptide stock solutions. Far-UV CD spectra in the range of 260 to 205-200 nm were acquired using a J-815 CD spectrometer from Jasco at a temperature of 25°C. The measurements were performed in the appropriate cuvette under a nitrogen flow, with a scanning interval of 1 nm, a spectral bandwidth of 2 nm, and a scanning velocity of 50 nm/min. Each spectrum represents an average of three scans, and buffer signals were subtracted from each scan to obtain the final spectra, **and the ellipticity was calculated as described in literature⁹.**

Regarding the **kinetic data analysis**, the analysis of kinetic experiment data conducted with P7 coacervates was done by subtracting the absorbances of P7 coacervates without pNPP and the absorbances over time of pNPP autohydrolysis in bulk. This approach helps account for background effects and isolates the catalytic activity of the coacervates.

To clarify this point, we added the following text to the revised manuscript in the section of the materials and methods under the section **Kinetic experiments of P7 the materials and methods**: The analysis of kinetic experiment data conducted with P7 coacervates involved two key corrections: (1) to account for the turbidity interference caused by coacervates, the absorbances of P7 coacervates without pNPP were subtracted from the experimental readings, and (2) to account for the autohydrolysis of the substrate in bulk solution, the absorbances of pNPP over time (without coacervates) were also subtracted from the experimental readings. These corrections allowed for a more accurate assessment of the catalytic activity of P7 coacervates by isolating the pNPP hydrolysis specifically caused by the peptide-based coacervates.

2. Coacervate can be formed with a secondary non-catalytic peptide that is then spiked with the P7 peptide. The P7 could therefore be at the same concentration as the bulky solution but the confirmation would be different.

Response: We appreciate the reviewer's suggestion. Our results demonstrate that the process of undergoing liquid-liquid phase separation (LLPS) is crucial for the peptide to adopt a defined beta-hairpin structure. We believe that encapsulating P7 peptides in coacervates formed by other peptides would constitute a fundamentally different system, requiring a more comprehensive investigation. Such an investigation would require:

1. Studying the interactions between the P7 peptide and the non-catalytic phase-separating peptide
2. Assessing the efficiency of P7 encapsulation

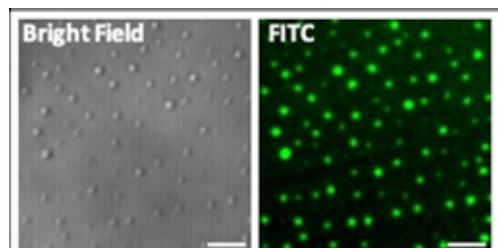
3. Analyzing the conformation of P7 within the new coacervate environment

The assessment of P7's conformation in this context would be particularly challenging due to the inevitable contribution of the non-catalytic phase-separating peptide to any structural analyses. One potential indirect approach would be to add P7 peptide at a final concentration where it typically exists as a flexible hairpin-like peptide. If encapsulation in the new coacervate environment also leads to the formation of a defined hairpin structure, we would expect to observe catalytic activity comparable to that obtained with P7 peptide-only coacervates. However, this approach would introduce additional variables and complexities that are beyond the scope of our current study, which focuses on the direct effects of LLPS on P7's structure and function.

For this, we have used a non-catalytic peptide, PJ1, which undergoes liquid-liquid phase separation (LLPS). This peptide was recently discovered in our lab as part of an ongoing project on phase-separating proteins. To maintain scientific integrity and avoid potential conflicts of interest, we will include these results only in this response and not in the main manuscript, as the peptide sequence is yet unpublished.

The PJ1 peptide (sequence: DGGGRYGGRPAP) is a rationally designed peptide incorporating tripeptide motifs YGG, GGR, and GGG, which are known to be enriched in intrinsically disordered proteins that undergo LLPS^{10, 11}.

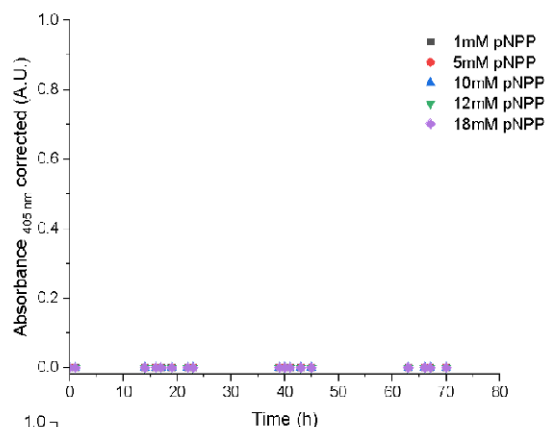
Our studies demonstrate that PJ1 undergoes LLPS under the same buffer conditions as P7 (100 mM sodium phosphate, pH 8.0, 1 M NaCl) and can partition FITC molecules similarly to P7 (Figure RRL2).



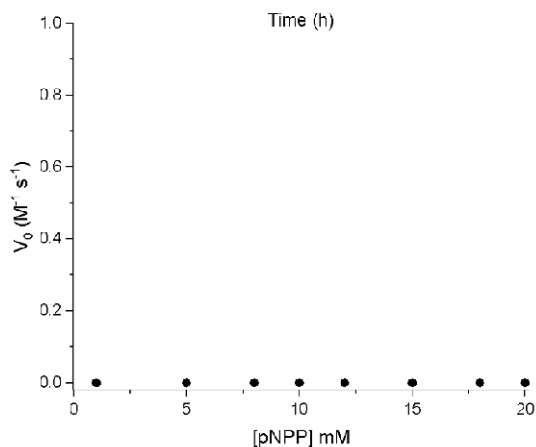
Reviewer Response Letter Figure 2: Confocal microscopy images showing the ability of PJ1 to undergo LLPS and form coacervates (a), and the partitioning of FITC in PJ1 coacervates (b). All scale bars: 10 μ m.

We performed partitioning experiments with P7 at a final concentration that will be the same concentration as the bulk of approximately 0.38 mg/mL, presenting a hairpin-like conformation. We also included pNPP at final concentrations of 1, 5, 10, 12, and 20 mM to conduct kinetic experiments of P7 coacervates towards pNPP. The results shown in Fig. RRL3 reveal no evidence of catalytic activity of P7 spiked in PJ1 coacervates towards pNPP. This lack of activity might indicate either the absence of a fully folded hairpin conformation of P7 within the PJ1 coacervates or the presence of additional variables affecting the catalytic function, as a result of a new system such as the possible interactions between P7 and PJ1, that could lead to interfere with the affinity towards the substrate.

a



b



Reviewer Response Letter Figure 3: The kinetic experiments of the PJ1 coacervates spiked with P7 peptide under bulky conditions (e.g., soluble) towards pNPP. The hydrolysis of the pNPP by the PJ1 coacervates spiked with P7 was monitored by the absorbance at 405 nm from the chromogenic product p-nitrophenol for a total of 90h. Data are presented as mean values \pm SD ($n = 3$).

The methodology used was the same as described in the main text of the manuscript for the partitioning protocol. For the kinetic experiments of PJ1 coacervates spiked with P7 pNPP, slightly challenges were included to partition simultaneously P7 and pNPP. In a cuvette, 186.4 μ L of the 5 mg/mL PJ1 peptide solution was mixed with 738.46 μ L of buffer and incubated for 5 minutes at 27°C (\pm 1°C) to induce coacervation. Subsequently, 38.46 μ L of P7 peptide from a 10 mg/mL stock solution was added, resulting in a final concentration of 0.38 mg/mL, the final concentration corresponding to the bulky solution, when the peptide is soluble. This was followed by the addition of 38.46 μ L of pNPP substrate for the final concentrations of 1, 5, 10, 12, and 20 mM, maintaining the ratios specified in the kinetics protocols. The samples were then incubated for 1 hour at 27°C (\pm 1°C). The formation of p-nitrophenol (pNP) was monitored by measuring the absorbance at 405 nm. The analysis of kinetic experiment data conducted with PJ1 coacervates spiked with P7 and pNPP involved two key corrections: (1) to account for the turbidity interference caused by coacervates, the absorbances of PJ1 coacervates without pNPP were subtracted from the experimental readings, and (2) to account for the autohydrolysis of the substrate in bulk solution, the absorbances of pNPP over time (without coacervates) were also subtracted from the experimental readings. These corrections allowed for a more accurate assessment of the catalytic activity of PJ1

coacervates spiked by isolating the pNPP hydrolysis specifically caused by the peptide-based coacervates.

3. Could buffer conditions (viscosity, etc) be optimized to show the conformational change of the P7 and improvement in kinetics.

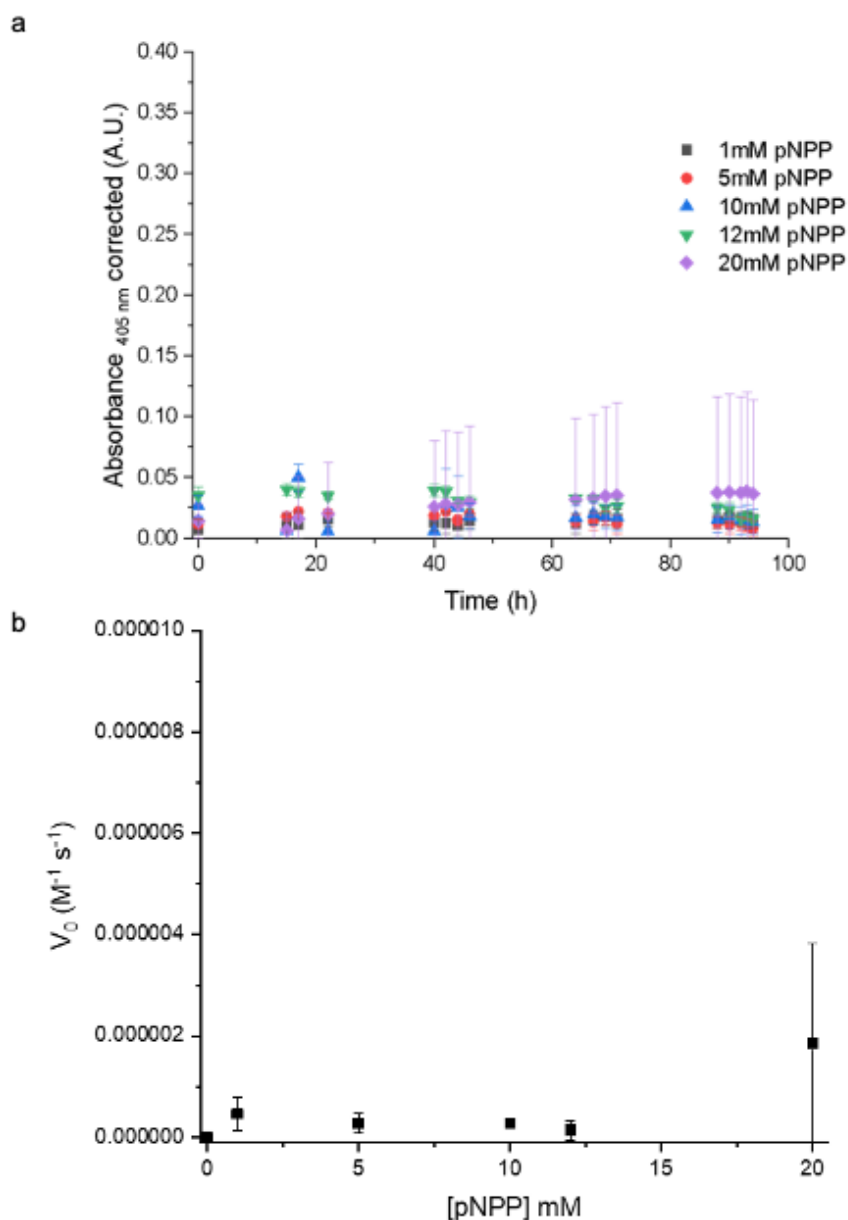
Response: We appreciate the reviewer's comment. We have studied different buffer conditions such as 100 mM sodium phosphate buffer at pH 8.0 with varying concentrations of NaCl (0 M, 0.25 M, and 1 M) to determine the best conditions to identify the optimal environment for P7 peptide to undergo liquid-liquid phase separation (LLPS), as shown in Figure 2.

Our findings indicate that the optimal condition for LLPS was in the presence of 1 M NaCl, suggesting that buffer viscosity can influence the LLPS of the peptide. While our primary focus was on the formation of coacervates and for further validation of the impact in catalysis, we acknowledge that further optimization of buffer conditions, including viscosity, could enhance our understanding of conformational stability and catalytic kinetics. In future studies, we can explore a broader range of buffer compositions to screen for conditions that may further improve the structural stability and catalytic efficiency of P7 coacervates. Thank you for your valuable suggestion, which will guide our future research efforts.

4. In general, the autocatalysis of the substrate in the coacervate needs to be demonstrated. Again, a non-catalytic coacervate peptide should be chosen for this control.

Response: We appreciate the reviewer's suggestion and have addressed it by utilizing a non-catalytic peptide, PJ1, which undergoes liquid-liquid phase separation (LLPS). This peptide was recently discovered in our lab as part of an ongoing project on phase-separating proteins. To maintain scientific integrity and avoid potential conflicts of interest, we will include these results only in this response and not in the main manuscript, as the peptide sequence is yet unpublished.

We performed kinetic experiments with PJ1 coacervates encapsulated with pNPP to elucidate the specific effects of pNPP autohydrolysis within coacervates. The results, shown in Figure RRL4, demonstrate that the autohydrolysis of pNPP once encapsulated inside the coacervates is lower and does not fit a Michaelis-Menten trend. This non-catalytic peptide serves as a valuable control, allowing us to distinguish between the catalytic activity of P7 and the background autohydrolysis of pNPP within the coacervate environment. These findings support our approach of subtracting the autohydrolysis of the substrate in bulk from the catalytic data and provide additional evidence for the specific catalytic activity of P7 coacervates.



Reviewer Response Letter Figure 4: The kinetic experiments of the PJ1 coacervates towards pNPP. The hydrolysis of the pNPP by the PJ1 coacervates was monitored by the absorbance at 405 nm from the chromogenic product p-nitrophenol for a total of 90h. Data are presented as mean values \pm SD ($n = 3$).

The methodology used was the same as described in the main text of the manuscript for the partitioning protocol and kinetic experiments of P7 coacervates towards p-nitrophenyl phosphate (pNPP).

5. I would like to see a bit more temperature data the 23 and 27 C seems like two arbitrary data points for the coacervation studies. Similarly, the kinetics at different temperatures would be beneficial.

Response: We appreciate the reviewer's comment regarding the temperature data. We agree that a more comprehensive temperature analysis would strengthen our study. In response, we have conducted a thorough investigation of coacervation at various

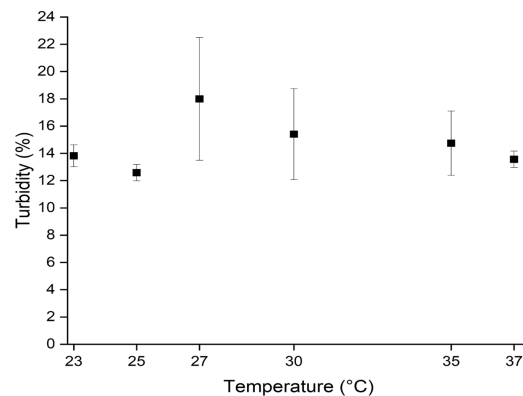
temperatures ranging from 23°C to 37°C under optimal conditions (stock peptide concentration of 5 mg mL⁻¹ in 100 mM sodium phosphate buffer, 1.00 M NaCl, pH 8), using both turbidity measurements and optical brightfield microscopy.

Our findings reveal that temperatures above 27°C show higher turbidity values (Figure S3), favoring coacervate formation compared to temperatures below 25°C (Figure S4). These results align with our previous coacervation studies conducted at 27°C and provide a more comprehensive understanding of the temperature-dependent behavior of our system.

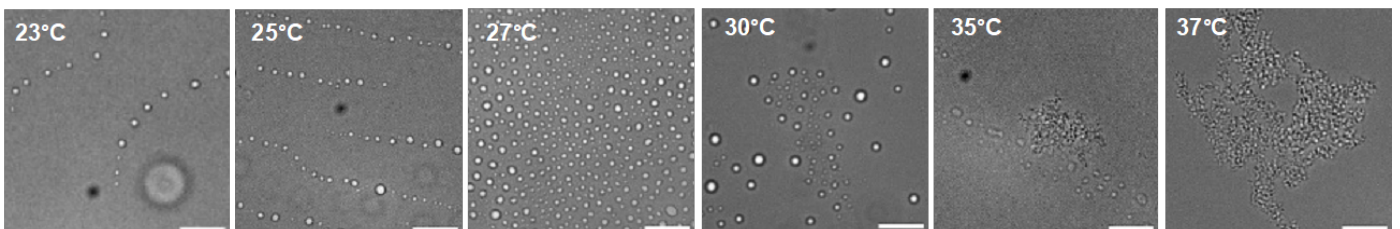
Interestingly, we observed that temperatures above 35°C led to aggregation, similar to the effects seen at higher peptide concentrations. This observation highlights the delicate balance between coacervation and aggregation in our system, which is influenced by both temperature and concentration.

Regarding the kinetic experiments, we acknowledge the reviewer's suggestion for temperature-dependent kinetics data. In our initial study, we conducted kinetics only at 25°C with p-nitrophenyl phosphate (pNPP) after inducing peptide coacervation at 27°C, to maintain comparability with our previous work on the P7 catalytic peptide in its soluble state.

We added the new results in Supplementary Fig. S3 and S4, and revised the text accordingly (page 7 lines 167-173):



Supplementary Figure 3 - Turbidity measurements of the stock P7 peptide concentration of 5 mg mL⁻¹, pH 8.0, and 1.0 M NaCl, 1h coacervation as a function of the temperature.



Supplementary Figure 4 - Influence of temperature ranging from 23°C to 37°C on coacervation formation using a stock P7 peptide concentration of 5 mg mL⁻¹, pH 8.0, and 1.0 M NaCl, for 1h. The scale bar is set to 10 μm.

Revised text: “To further elucidate this process, we investigated the impact of temperature on P7 coacervation under optimal conditions (stock peptide concentration of 5 mg mL⁻¹ in 100 mM sodium phosphate buffer, 1.00 M NaCl, pH 8), using turbidity measurements and optical

brightfield microscopy (Supplementary section 2.2). We assessed different temperatures ranging from 23°C to 37°C. Coacervate formation was observed within one hour of incubation, with temperatures above 27°C showing higher turbidity values (Figure S3), favoring coacervate formation compared to temperatures below 25°C (Figure S4). These data are consistent with previous studies on similar systems where coacervation is primarily driven by hydrophobic interactions, which are known to be temperature-sensitive²⁵. Similar to the effects of higher peptide concentrations, higher coacervation temperatures (>35°C) also led to aggregation.”

6. For the supplementary info in part 3 where you are looking at the partitioning. I think the result is interesting, but it does seem like different enzyme/dye to peptide ratios need to be studied for a proper analysis.

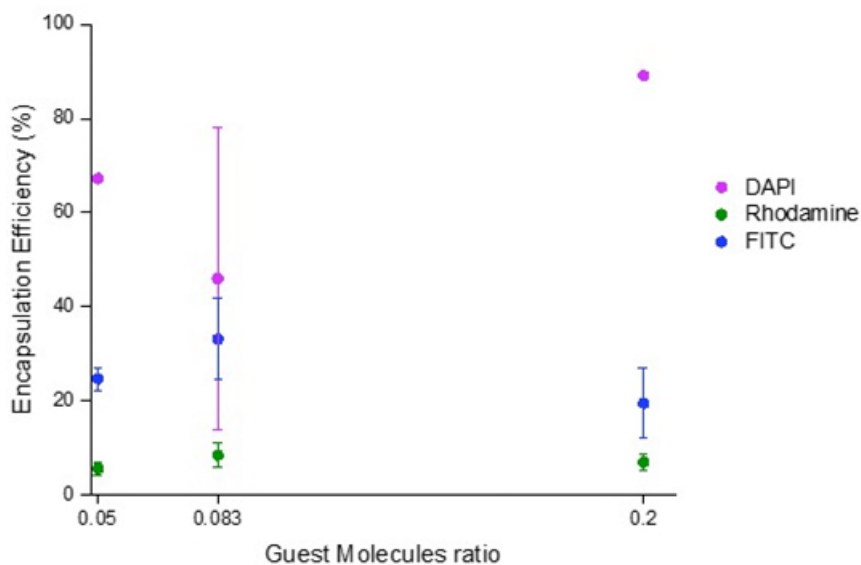
Response: We appreciate the reviewer's insightful suggestion regarding the study of different enzyme/dye to peptide ratios. In response, we have conducted a comprehensive analysis of P7 coacervates using various P7-to-guest molecule ratios (1:5, 1:12, and 1:20). Our findings reveal intriguing patterns in the partitioning behavior of guest molecules. For hydrophobic molecules such as FITC and Rhodamine, the partitioning is largely independent of concentration, suggesting that the hydrophobic interactions, governed by the P7 peptide sequence, play a dominant role. The peptide creates a specific hydrophobic environment that selectively attracts these molecules. For less hydrophobic molecules (e.g., DAPI), the partitioning efficiency increases with higher peptide:guest molecule ratios. This indicates that additional interactions, such as hydrogen bonding, may be involved. At pH 8.0, where both peptide coacervates and guest molecules have the same charge, electrostatic interactions are likely minimal. This comprehensive analysis not only addresses the reviewer's concern but also provides deeper insights into the complex interplay of interactions governing molecular partitioning in our peptide-based coacervate system.

We added the new results in Supplementary Fig.13, and revised the text accordingly (page 11 lines 264-270):

Different ratios of the peptide P7-to-guest molecule ratio were used (Fig. S8). Our findings reveal that for hydrophobic molecules such as FITC and Rhodamine, the partitioning is largely independent of concentration, suggesting that hydrophobic interactions, governed by the P7 peptide sequence, play a dominant role. For less hydrophobic molecules like DAPI, the partitioning efficiency increases with higher peptide-to-guest molecule ratios. This indicates that additional interactions, such as hydrogen bonding, may be involved.

We then used fluorescence recovery after photobleaching (FRAP) to characterize the dynamics of coacervates, with FITC as a representative guest molecule (Figs. 3c-3d). Our results demonstrate a significant (~60%) fluorescence recovery in the coacervates, affirming their liquid-like nature.

Collectively, these observations demonstrate that P7 coacervates selectively control the dynamic partitioning of guest molecule and suggest that π - π interactions between the aromatic groups of the dye molecules and the aromatic residues of the P7 peptide together with hydrogen bonding between the peptide and less hydrophobic guest molecules mediate partitioning within the coacervates. Therefore, the functional properties of peptide coacervates are intricately tied to the encoded peptide sequence, which influences the partitioning of molecules within the coacervates.



Supplementary Figure 13 – Encapsulation efficiency (%) of guest molecules as a function of the peptide-to-guest molecule ratio in P7 coacervates. Different peptide-to-guest molecule ratios were tested, including 1:5, 1:12, and 1:20. The encapsulation efficiency was determined by measuring the partitioning of the guest molecules within the coacervates. Data are presented as mean values \pm SD (n=3).

Minor issues:

7. Can the aggregates be tested for catalytic activity?

Response: We appreciate the reviewer's suggestion to evaluate the catalytic activity of the aggregates. However, testing the aggregates for catalytic activity presents significant challenges:

1. Optical interference: The aggregates can reach absorbance values higher than 2 A.U. at 405 nm, which is beyond the reliable range for spectrophotometric measurements. This high absorbance would interfere with accurate quantification of the catalytic reaction products.
2. Sample heterogeneity: The amorphous nature of the aggregates leads to inconsistent sample composition, making it difficult to obtain reproducible results or make valid comparisons with the P7 coacervates.
3. Limited accessibility: The dense, irregular structure of aggregates (as shown in Figure 2) likely restricts substrate access to potential catalytic sites, potentially masking any inherent activity.

Given these limitations, we believe that direct measurement of catalytic activity in the aggregate samples would not yield reliable or comparable results. Based on the amorphous nature of these aggregates and their structural characteristics, we hypothesize that they would exhibit little to no catalytic activity

8. There are some formatting issues, particularly when equations are involved with subscript, etc.

Response: Thank you for bringing this to our attention. We will make these corrections and submit a revised version with improved formatting.

9. I think the authors overplay some phrases in the introduction. For example: “In any event, the potential use of peptides to induce coacervate formation is yet to be fully recognized.” is pretty silly when there are special issues dedicated to the topic and all sorts of publications coming out all the time. I would ask that the authors reconsider some of the hyperbole.

Response: We appreciate the reviewer's feedback and understand the concern regarding the phrasing used in the introduction.

We acknowledge that the field of peptides inducing coacervate formation is well-established, with numerous publications and special issues dedicated to this topic. Therefore, we will revise the introduction to ensure it accurately reflects the current state of research without overstating our claims. Specifically, we will remove the phrase “In any event, the potential use of peptides to induce coacervate formation is yet to be fully recognized” to better align with the extensive body of work in this area.

We have revised the text accordingly (page 3 lines 83-87):

Exploring this mechanism further, minimal model systems of self-coacervation have been developed using specifically designed peptides that adhere to these principles^{12, 13, 14, 15}. One of the major challenges in developing coacervates from simple building blocks that simultaneously govern condensate organization and mediate predictable functionality remains largely unaddressed¹⁶.

10. In a similar vein, I feel the work of the Elbaum-Garfinkle and Ulijn groups in peptide coacervates has been overlooked. I recommend the authors look at:

- a. <https://onlinelibrary.wiley.com/doi/full/10.1002/anie.202218067>
- b. <https://www.sciencedirect.com/science/article/pii/S245192942200153X>
- c. <https://onlinelibrary.wiley.com/doi/abs/10.1002/ange.202311479>
- d. <https://www.nature.com/articles/s41467-020-18224-y>

Response: We appreciate the reviewer's suggestion regarding the need to reference relevant works in the field of liquid-liquid phase separation (LLPS) and peptides. We apologize for not including these significant contributions in our initial submission. We aim to provide a balanced representation that acknowledges the substantial advancements made by previous studies while highlighting the unique aspects and contributions of our research. To address this, we have revised the manuscript to include the mentioned works and ensure that our discussion accurately reflects the current state of research in LLPS and peptides. The relevant references have been added to the text on page 3, lines 80-85.

While the mechanisms by which LLPS enables membraneless organelle formation are still being elucidated, previous studies have highlighted the importance of uncharged polar side chains, charged amino acids, and aromatic residues located in the repetitive low-complexity regions of intrinsically disordered proteins for coacervation^{1,3,4}. Exploring this mechanism further, minimal model systems of self-coacervation have been developed using specifically designed peptides that adhere to these principles^{12, 13, 14, 15, 17, 18}.

Reviewer #4 (Remarks to the Author):

This is an interesting study with great potential. However, there are several concerns that need to be addressed.

Response: We appreciate the reviewer's constructive feedback and have addressed each comment in detail below.

1. Applicability of CD for structural analysis of aggregated protein samples and samples that underwent LLPS is questionable. Results are undoubtedly affected by light scattering. Therefore, reported spectral shapes (and the complete lack of signal for aggregated protein) should not be used for any structural interpretations. Instead (e.g., FTIR), which are not sensitive to the artifacts generated by aggregation, should be used for structural characterization of E7 peptide under the variety of conditions.

Response: We appreciate the reviewer's concern regarding the applicability of CD for structural analysis of aggregated protein samples and those undergoing LLPS. To address this, we have employed FTIR spectroscopy as a complementary method to identify the secondary structure of the P7 peptide across various assembly states.

The FTIR spectra shown in Figure S8 reveal distinct differences in the amide I band region, indicative of secondary structure variations. To precisely determine the contribution of each secondary structure, we deconvoluted the amide I band using a nonlinear Gaussian curve fit in OriginPro 2024b software. Deconvolution of the amide I band in the soluble state (Figure S9a and Table S2) primarily indicates the presence of a random coil conformation (band at 1640 cm^{-1}), with a minor band at 1685 cm^{-1} attributed to a β -turn, reinforcing the presence of a hairpin-like peptide structure.

In the P7 coacervates, the β -sheet conformation was significantly higher, accounting for approximately 70% of the structure (Figure S9a, S9d, and Table S2). This was evidenced by the contributions of β -sheet bands at 1623 cm^{-1} and 1663 cm^{-1} , along with a β -turn band at 1683 cm^{-1} , thus reinforcing the presence of a β -hairpin structure in the LLPS state. Conversely, in the aggregated assembly state (Figure S9c and Table S2), there is a significant decrease in β -sheet content (down to 20%) (Figure S9d) compared to the P7 coacervates, with a more pronounced random coil conformation, corroborating a loss of conformational order.

These FTIR findings are consistent with the results obtained from CD and NMR analyses, indicating an enhanced content of β -sheet and higher structural organization in P7 coacervates compared to the soluble and aggregated states. Collectively, these structural investigations underscore the critical role of LLPS in modulating the conformational flexibility of the P7 peptide, stabilizing structured domains.

In summary, the FTIR results corroborate our findings from CD and NMR, providing a comprehensive understanding of the structural transitions of the P7 peptide in different assembly states. The use of FTIR has allowed us to overcome the limitations posed by light scattering in CD, ensuring precise structural characterization. This reinforces the importance of LLPS in enhancing the functional properties of the P7 peptide through structural organization.

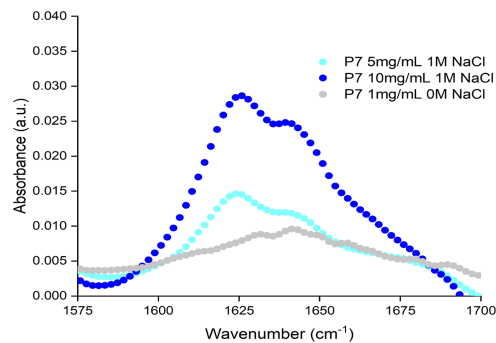
We added the new results in Supplementary Fig. 8 and 9, Table S2 and revised the text accordingly (page 8 lines 203-221):

Fourier-transform infrared (FTIR) spectroscopy was employed as a complementary method to identify the secondary structure of the P7 peptide in various assembly states. The FTIR spectra, shown in Figure S8 reveal distinct differences in the amide I band region, indicative of secondary structure variations. Deconvolution of the amide I band in the soluble state (Figure S9a and Table S2) primarily indicates the presence of a random coil conformation (band at 1640 cm^{-1}), with a minor band at 1685 cm^{-1} attributed to a β -turn¹⁹, reinforcing the presence of a hairpin-like peptide structure.

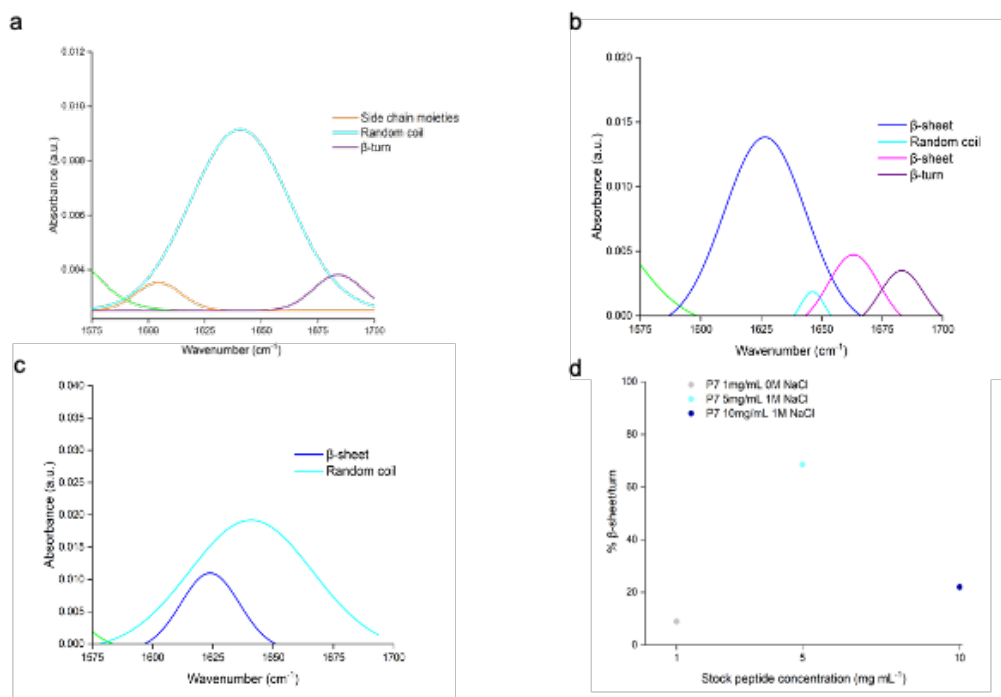
In the P7 coacervates, the β -sheet conformation was significantly higher, accounting for approximately 70% of the structure (Figure S9a, S9d and Table S2). This was evidenced by the contributions of β -sheet bands at 1623 cm^{-1} and 1663 cm^{-1} , along with a β -turn band at 1683 cm^{-1}

^{19, 20}, thus reinforcing the presence of a β -hairpin structure in the LLPS state. Conversely, in the aggregated assembly state (Figure S9c and Table S2), there is a significant decrease in β -sheet content (down to 20%) (Figure S9d) compared to the P7 coacervates, with a more pronounced random coil conformation, corroborating a loss of conformational order.

These FTIR findings are consistent with the results obtained from CD and NMR analyses, indicating an enhanced content of β -sheet and higher structural organization in P7 coacervates compared to the soluble and aggregated states. Collectively, these structural investigations underscore the critical role of LLPS in modulating the conformational flexibility of the P7 peptide, stabilizing structured domains.



Supplementary Figure 8: FTIR spectra of the peptide in three distinct assembly states: soluble (1 mg mL^{-1} , undergoing LLPS (5 mg mL^{-1} 1 M NaCl), and in the aggregate (10 mg mL^{-1} 1 M NaCl)



Supplementary Figure 9: Deconvolution of the amide band I peak of P7 in the various states: (a) soluble state (P7 stock concentration 1 mg mL^{-1} with no salt), (b) undergoing LLPS (stock concentration 5 mg mL^{-1} 1 M NaCl) and, (c) aggregated state (10 mg mL^{-1} 1 M NaCl). (d) Percentage of β -sheet and β -turn content in the different assembly states, calculated from the areas of peaks corresponding to β -sheet (1623 cm^{-1} and 1663 cm^{-1}) and β -turn (1683 cm^{-1}) structures, divided by the total area of all peaks in the amide I region.

Supplementary Table 2 – Vibrational frequencies (cm^{-1}) of the absorption bands associated with secondary structure conformation of the various states of P7 in the Amide I band.

Assembly state	Vibrational frequency range (cm^{-1})	Maximum Peak (cm^{-1})	Structural assignment
Soluble (P7 1mg/mL with no salt)	1597-1609	1605	Side chain moieties
	1634-1650	1640	Random Coil
	1679-1687	1685	β -turn
	1622-1631	1622	β -sheet
LLPS (P7 5mg/mL 1M NaCl)	1643-1648	1646	Random coil
	1660-1667	1663	β -sheet
	1679-1689	1683	β -turns
	1618-1630	1623	β -sheet
Aggregated (P7 10mg/mL 1M NaCl)	1633-1648	1640	Random Coil

The materials and methods section were also updated accordingly with this new data, and we added the following text: **FTIR spectroscopy:** Attenuated total reflection (ATR)-FTIR measurements were performed using a zinc-selenide crystal with a 45° angle of incidence. Samples of P7 peptide were prepared according to the coacervation protocol at three concentrations: 1 mg mL^{-1} in 100 mM sodium phosphate buffer pH 8.0 without salt (soluble), 5 mg mL^{-1} in the same buffer with 1 M NaCl (undergoing LLPS), and 10 mg mL^{-1} in the same buffer with 1 M NaCl. $10 \mu\text{L}$ of each sample was analyzed. ATR-FTIR spectra were recorded in the amide I band ($1550\text{-}1720 \text{ cm}^{-1}$) with a spectral resolution of 4 cm^{-1} using a Bruker INVENIO R spectrometer equipped with a DTGS detector. Measurements were conducted at room temperature while purging the sample compartment with dry air. Each spectrum comprised 64 scans, was baseline corrected, and the amide I band was deconvoluted using OriginPro 2024b software.

2. More focus should be given to NMR-based analyses.

Response: As recommended by the reviewer, we have conducted a more comprehensive NMR-based analyses The NMR data was thoroughly examined, revealing significant insights into the structural changes of P7 during LLPS. Our results provide strong evidence that LLPS induces the stabilization of the secondary structure of P7, transforming it from a flexible hairpin-like peptide in solution to a fully folded β -hairpin structure in the LLPS state. For a detailed discussion of these findings, please refer to our response to reviewer #2, comment#1.

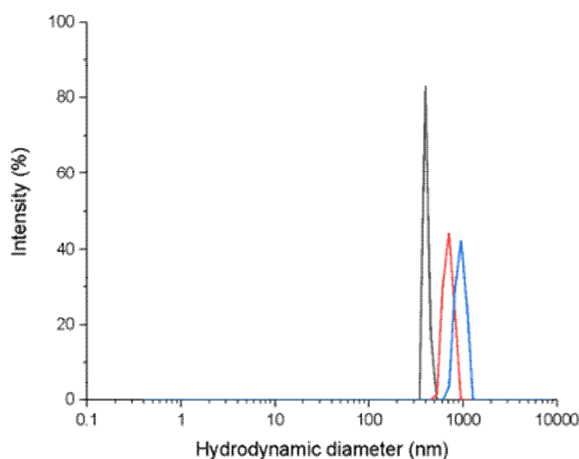
3. Sequence of the analyzed peptide is rather hydrophobic. Potentially, it never exists as a monomer. Some analysis of the association state of the "soluble" sample should be conducted.

Response: We appreciate the reviewer's insightful observation regarding the hydrophobic nature of the peptide sequence. We agree that our initial characterization of the "soluble" state could benefit from further clarification and analysis. To address this, we have conducted additional experiments to better understand the association state of the peptide under conditions where no visible coacervates or turbidity are observed.

Dynamic Light Scattering (DLS) measurements were performed on the "soluble" sample (1 mg/mL peptide in 100 mM sodium phosphate buffer, pH 8.0, with no salt NaCl). The results revealed a range of hydrodynamic diameters between 500 to 1000 nm, indicating the presence of soluble associations rather than monomeric peptides. This finding aligns with

the reviewer's suggestion that the peptide may not exist solely as monomers due to its hydrophobic nature.

We acknowledge that our use of the term "soluble state" in the manuscript may have been imprecise. To clarify, we use this term to describe conditions where the sample exhibits low turbidity and a limited number of visible coacervates, rather than implying a truly monomeric state. The main focus of our study was to correlate the transition from this "soluble" (low turbidity) state to the LLPS state with changes in the peptide's secondary structure and catalytic activity.



We have revised the text accordingly (page 7 lines 188-200):

The secondary structure of the peptide was analyzed in three distinct assembly states: soluble (any of the conditions 1 mg mL^{-1} with no salt, 5 mg mL^{-1} with no salt or 1 mg mL^{-1} with 1 M NaCl showing absence or low turbidity), undergoing LLPS (5 mg mL^{-1} 1 M NaCl), and in the aggregate (10 mg mL^{-1} 1 M NaCl)

4. There is no any evidence showing that P7 has a flexible hairpin-like structure in soluble form. Formation of a fully folded β -hairpin structure is not supported by data provided.

Response: We appreciate the reviewer's concern regarding the evidence for P7's flexible hairpin-like structure in the soluble form and its transition to a fully folded β -hairpin structure during LLPS. To address this, we have conducted comprehensive analyses using both NMR and FTIR techniques, which provide robust support for our findings. Our enhanced NMR analysis reveals significant chemical shift changes between the soluble and LLPS states, indicating a transition from a flexible structure to a more ordered conformation. The FTIR measurements further corroborate these results, showing distinct differences in the amide I band region that are consistent with the formation of a β -hairpin structure in the LLPS state.

These complementary techniques provide strong evidence for the structural transition of P7 from a flexible hairpin-like peptide in solution to a fully folded β -hairpin structure in the LLPS state. For a detailed discussion of these findings, including specific spectral data and their interpretation, please refer to our response to reviewer #2, comment #1, and to comment #1 of this section.

5. What was phosphorylation degree of proteins used in this study?

Response: We thank the reviewer for this important comment. The BSAp and Taup proteins used in our study are commercially available. However, their phosphorylation degree is not specified in the product information. Given that these proteins are certified for quality, we believe that the phosphorylation degree is as high as possible. This assumption is supported by the SDS-PAGE analysis, where we observe a distinct increase in molecular weight for Taup compared to Tau (45.9 kDa versus 64-70 kDa) shown in the product specifications, indicating significant phosphorylation. The same observation for BSA and BSAp (66.43 kDa versus 68.33 kDa). For the CotB protein, the phosphorylation degree is approximately 100%, as reported in previous work ⁶

To provide comprehensive information about the commercially used proteins, we have included their references in the supplementary section under the Materials topic. This ensures that all relevant details are readily accessible for readers: **BSAp (phosphorylated Bovine Serum Albumin, FITC-Labelled BSA - P3967, Human microtubule associated protein tau, Tau-441 - T0576, Tau-44p - TTBK1-Phosphorylated - SRP0695.**

6. The authors mentioned that in their experiments on the catalytic efficiency, no observable hydrolysis of pNPP occurred even after 90 hours was found without coacervation. However, previous study showed that this peptide is catalytically active "in a bulk solution under catalytic optimal conditions". The authors should indicate what is the difference between the conditions used in their study and previously reported "catalytic optimal conditions". Can coacervates be formed at these "catalytic optimal conditions"?

Response: We thank the reviewer for this important comment and appreciate the opportunity to clarify our experimental conditions. In our current study, we examined the P7 peptide under two conditions:

1. Coacervate form: 5 mg/mL stock concentration in 100 mM sodium phosphate buffer (pH 8.0) with 1 M NaCl. Coacervation was induced by adding peptide to buffer in a 1:5 ratio at 27°C.
2. Bulk solution: The same buffer conditions as above, but without inducing coacervation, resulting in a final peptide concentration of 1 mg/ml.

In the bulk solution condition, we observed no catalytic activity even after 90 hours.

The "catalytic optimal conditions" referred to in Pina et al. (2022)¹ were different:

- Final peptide concentration: 50 μ M
- Buffer: 100 mM sodium phosphate (pH 8.0)
- No additional salt

Under these conditions, the peptide was catalytically active in bulk solution. The key differences between our current study and the previously reported optimal conditions are: Peptide concentration (1 mg/mL vs 50 μ M), Presence of 1 M NaCl in our current study and temperature (27°C), which are crucial to induce coacervation.

Regarding coacervate formation under the "catalytic optimal conditions," we have not specifically tested this. However, based on our phase diagram studies, coacervate formation is unlikely under those conditions due to the absence of salt and the lower peptide concentration. These differences in conditions explain the discrepancy in

catalytic activity observed between the two studies and highlight the importance of the coacervate state for enhancing the peptide's catalytic efficiency.

In order to improve the clarity of the revised manuscript, we have modified the following text:

Pages 14, lines 352-354: In the condition without triggering coacervation, we dissolved the peptide in the same buffer solution to achieve the same final concentration of 1 mg mL⁻¹. **This concentration was selected to correspond with the final peptide concentration in the coacervate samples, while maintaining the peptide in a soluble state and preventing phase separation.** The substrate was then added to the resulting solution, and the catalytic reaction was also conducted at 27°C (Fig. 5b). Without coacervation, no observable hydrolysis of pNPP occurred even after 90 hours.

Pages 15, lines 354-355: The comparison between the kinetic parameters obtained with P7 peptide-based coacervates to those previously determined for the peptide P7 in a bulk solution under catalytic optimal conditions (**i.e., P7 final concentration of 50µM in 100 mM sodium phosphate pH 8.0 with no salt, and catalytic reaction temperature 25 °C**)¹.

References

1. Pina AS, Morgado L, Duncan KL, Carvalho S, Carvalho HF, Barbosa AJM, *et al.* Discovery of phosphotyrosine-binding oligopeptides with supramolecular target selectivity. *Chemical Science* 2022, **13**(1): 210-217.
2. Cakmak FP, Choi S, Meyer MO, Bevilacqua PC, Keating CD. Prebiotically-relevant low polyion multivalency can improve functionality of membraneless compartments. *Nature Communications* 2020, **11**(1): 5949.
3. Choi S, Knoerdel AR, Sing CE, Keating CD. Effect of Polypeptide Complex Coacervate Microenvironment on Protonation of a Guest Molecule. *The Journal of Physical Chemistry B* 2023, **127**(26): 5978-5991.
4. Schindelin J, Arganda-Carreras I, Frise E, Kaynig V, Longair M, Pietzsch T, *et al.* Fiji: an open-source platform for biological-image analysis. *Nature Methods* 2012, **9**(7): 676-682.
5. van Veldhuisen TW, Altenburg WJ, Verwiel MAM, Lemmens LJM, Mason AF, Merckx M, *et al.* Enzymatic Regulation of Protein–Protein Interactions in Artificial Cells. *Advanced Materials* 2023, **35**(29): 2300947.
6. Freitas C, Plannic J, Isticato R, Pelosi A, Zilhão R, Serrano M, *et al.* A protein phosphorylation module patterns the *Bacillus subtilis* spore outer coat. *Molecular Microbiology* 2020, **114**(6): 934-951.
7. Lee W, Rahimi M, Lee Y, Chiu A. POKY: a software suite for multidimensional NMR and 3D structure calculation of biomolecules. *Bioinformatics* 2021, **37**(18): 3041-3042.

8. Hafsa NE, Arndt D, Wishart DS. CSI 3.0: a web server for identifying secondary and super-secondary structure in proteins using NMR chemical shifts. *Nucleic Acids Research* 2015, **43**(W1): W370-W377.
9. Greenfield NJ. Using circular dichroism spectra to estimate protein secondary structure. *Nature Protocols* 2006, **1**(6): 2876-2890.
10. Villegas JA, Heidenreich M, Levy ED. Molecular and environmental determinants of biomolecular condensate formation. *Nature Chemical Biology* 2022, **18**(12): 1319-1329.
11. Calabretta S, Richard S. Emerging Roles of Disordered Sequences in RNA-Binding Proteins. *Trends in Biochemical Sciences* 2015, **40**(11): 662-672.
12. Sun Y, Lau SY, Lim ZW, Chang SC, Ghadessy F, Partridge A, *et al.* Phase-separating peptides for direct cytosolic delivery and redox-activated release of macromolecular therapeutics. *Nature Chemistry* 2022, **14**(3): 274-283.
13. Abbas M, Lipiński WP, Nakashima KK, Huck WTS, Spruijt E. A short peptide synthon for liquid–liquid phase separation. *Nature Chemistry* 2021, **13**(11): 1046-1054.
14. Baruch Leshem A, Sloan-Dennison S, Massarano T, Ben-David S, Graham D, Faulds K, *et al.* Biomolecular condensates formed by designer minimalistic peptides. *Nature Communications* 2023, **14**(1): 421.
15. Tang Y, Bera S, Yao Y, Zeng J, Lao Z, Dong X, *et al.* Prediction and characterization of liquid-liquid phase separation of minimalistic peptides. *Cell Reports Physical Science* 2021, **2**(9): 100579.
16. Dai Y, Farag M, Lee D, Zeng X, Kim K, Son H-i, *et al.* Programmable synthetic biomolecular condensates for cellular control. *Nature Chemical Biology* 2023, **19**(4): 518-528.
17. Fisher RS, Elbaum-Garfinkle S. Tunable multiphase dynamics of arginine and lysine liquid condensates. *Nature Communications* 2020, **11**(1): 4628.
18. Sementa D, Dave D, Fisher RS, Wang T, Elbaum-Garfinkle S, Ulijn RV. Sequence-Tunable Phase Behavior and Intrinsic Fluorescence in Dynamically Interacting Peptides. *Angewandte Chemie International Edition* 2023, **62**(50): e202311479.
19. bagińska K, Makowska J, Wiczak W, Kasprzykowski F, Chmurzyński L. Conformational studies of alanine-rich peptide using CD and FTIR spectroscopy. *Journal of Peptide Science* 2008, **14**(3): 283-289.



20. Barreto MSC, Elzinga EJ, Alleoni LRF. The molecular insights into protein adsorption on hematite surface disclosed by in-situ ATR-FTIR/2D-COS study. *Scientific Reports* 2020, **10**(1): 13441.

REVIEWERS' COMMENTS

Reviewer #1 (Remarks to the Author):

The authors have extensively and adequately answered all the reviewers' comments. The paper is now suited for publication.

Response: We thank the reviewer for the positive and constructive feedback.

Reviewer #2 (Remarks to the Author):

The authors have addressed all my comments and concerns in their revision. I would now recommend publication.

Response: We thank the reviewer for the positive and constructive feedback.

Reviewer #3 (Remarks to the Author):

I commend the authors for undertaking considerable work to improve the manuscript and to make things clearer to a reader, where pertinent they have realized the suggested experiments and where not feasible they have provided an adequate explanation. I believe the manuscript is ready to be accepted for publication.

Response: We thank the reviewer for the positive and constructive feedback.

Reviewer #4 (Remarks to the Author):

All my concerns were adequately addressed, and the manuscript was revised accordingly. I do not have new queries.

Response: We thank the reviewer for the positive and constructive feedback.

Comments on “Catalytic Peptide-based Coacervates: Evolutionary Paths for Enhanced Catalytic Function through Structural Organization and Substrate Specificity” by Reis *et al.*

Summary

In this manuscript, the authors investigate the role of LLPS in enhancing the catalytic efficiency and substrate specificity of peptide P7. They showed that LLPS-mediated droplets not only exhibit a 15000-fold in enzymatic activity compared to non-phase separated soluble peptides, but can also selectively sequester phosphorylated substrates compared to non-phosphorylated substrates. In the course their research, they used a combination of enzyme catalysis studies and biophysical techniques including light scattering, microscopy, CD and NMR spectroscopy. They show that the self-coacervation of peptide P7 is reversible, and is dependent on solution conditions such as salt concentration and P7 concentration. However, under certain conditions, aggregates form. Their CD spectroscopy experiments demonstrate some conformational transition changes from a flexible disordered structure to beta-hairpin conformation. The changes in NMR spectroscopy chemical shift changes also reflect some conformational changes accompanying phase separation. To investigate the milieu formed within these P7 droplets, the authors investigated the sequestration and dynamics of aromatic dyes rhodamine, FITC and DAPI as well as GFP. They showed that less hydrophobic and negatively charged dyes as well as phosphorylated substrates are more encapsulated within the P7 coacervates.

Taken together, the authors demonstrates the ability of peptides to form both membrane-less droplets and to catalyze reactions with enhanced activity and selectivity. This paper will be of interest to the general readers of Nature Communication.

General Comments: The manuscript was well-written and organized, and straight forward to read and follow. In the attached documents, I have included specifics comments to help improve the documents.

Major Concern: I have only one major issue concerning the interpretation of the CD and NMR spectroscopy results. On line 97-99 of the manuscript, the authors wrote “Then, we demonstrate that coacervation reduces the conformational flexibility of the peptide, stabilizing a fully folded β -hairpin structure”. However, if there was there such significant structural change upon phase separation, the NMR chemical shift changes would have been more dramatic. I think without performing assignment experiments of the two states, it will be very difficult to just that statement. It’s feasible that the CD is detecting only partial folded Beta-hairpin structures.

Minor Comments: Maybe if the authors can speculate about the origin of the substrate specificity for phosphorylated vs non-phosphorylation substrates, that would be great.

I think this manuscript should be considered for publication after addressing these.